ACS APPLIED MATERIALS & INTERFACES

Research Article

www.acsami.org

Engineering a Dual-Layer Chitosan–Lactide Hydrogel To Create Endothelial Cell Aggregate-Induced Microvascular Networks In Vitro and Increase Blood Perfusion In Vivo

Sungwoo Kim,[†] Toshiyuki Kawai,[†,‡] Derek Wang,[§,⊥] and Yunzhi Yang*[,†,§,⊥]

[†]Department of Orthopedic Surgery, [§]Department of Materials Science and Engineering, and [⊥]Department of Bioengineering, Stanford University, 300 Pasteur Drive, Stanford, California 94305, United States

[‡]Department of Orthopedic Surgery, Kyoto University, 54 Kawaharacho, Shogoin, Sakyo-ku Kyoto 606-8507, Japan

ABSTRACT: Here, we report the use of chemically cross-linked and photo-cross-linked hydrogels to engineer human umbilical vein endothelial cell (HUVEC) aggregate-induced microvascular networks to increase blood perfusion in vivo. First, we studied the effect of chemically cross-linked and photo-cross-linked chitosan–lactide hydrogels on stiffness, degradation rates, and HUVEC behaviors. The photo-cross-linked hydrogel was relatively stiff (E = ∼15 kPa) and possessed more compact networks, denser surface texture, and lower enzymatic degradation rates than the relatively soft, chemically cross-linked hydrogel (E = ∼2 kPa). While both hydrogels exhibited nontoxicity, the soft chemically cross-linked hydrogels expedited the formation of cell aggregates compared to the photo-cross-linked hydrogels. Cells on the less stiff, chemically cross-linked hydrogels expressed more matrix metalloproteinase (MMP) activity than the stiffer, photo-cross-linked hydrogel. This difference in MMP activity resulted in a more dramatic decrease in mechanical stiffness after 3 days of incubation for the chemically cross-linked hydrogel, as compared to the photo-cross-linked one. After determining the physical and biological properties of each hydrogel, we accordingly engineered a dual-layer hydrogel construct consisting of the relatively soft, chemically cross-linked hydrogel layer for HUVEC encapsulation, and the relatively stiff, acellular, photo-cross-linked hydrogel for retention of cell-laden microvasculature above. This dual-layer hydrogel construct enabled a lasting HUVEC aggregate-induced microvascular network due to the combination of stable substrate, enriched cell adhesion molecules, and extracellular matrix proteins. We tested the dual-layer hydrogel construct in a mouse model of hind-limb ischemia, where the HUVEC aggregate-induced microvascular networks significantly enhanced blood perfusion rate to ischemic legs and decreased tissue necrosis compared with both no treatment and nonaggregated HUVEC-loaded hydrogels within 2 weeks. This study suggests an effective means for regulating hydrogel properties to facilitate a stable, HUVEC aggregate-induced microvascular network for a variety of vascularized tissue applications.

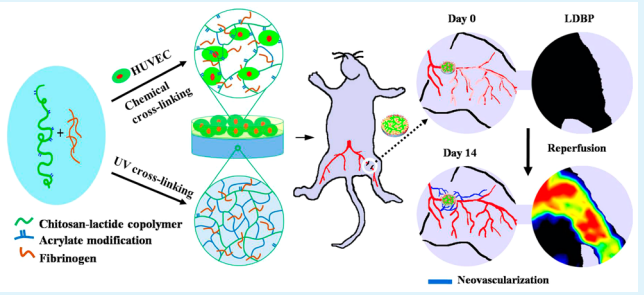

KEYWORDS: *chitosan, lactide, fibrinogen, hydrogel, HUVECs, aggregates, prevascularization, angiogenesis, hind-limb ischemia*

1. INTRODUCTION

Cell-based angiogenic therapeutics, including cell-laden hydrogel delivery, hold great promise for the treatment of vascular diseases or damaged vascularized tissues.[1−6] However, these approaches are limited by poor engraftment of cells due to the lack of functional vasculature. This is because the complex formation and regression of endothelial vascular networks are highly dependent on appropriate spatiotemporal microenvironmental cues in vitro and in vivo.[3,6−8] Mimicking the microenvironments in the engineered tissues still remains a significant technological challenge.[9]

It is well-known that extracellular matrix (ECM) can dynamically control cell survival, proliferation, migration, and differentiation,[10−14] and ECM itself is further remodeled by cell activities.[14−17] ECM mainly consists of laminins, collagen IV (Col IV), fibronectin, perlecan, nidogens, and collagen XVIII.[15−17] Among ECM proteins, Col IV provides the major structural support and is frequently colocalized with fibronectin,[17] while fibronectin has high binding affinity to angiogenic factors, such as vascular endothelial growth factor, thereby enhancing endothelial cells (EC) growth, migration, and tubulogenesis.[16] During vascular remodeling, the matrix metalloproteinases (MMPs)-mediated degradation of the ECM is essential for vessel formation and regression.[14,18,19] Increased MMP activity of ECs is responsible for excessive degradation and local accumulation of the decomposed ECM components.[18,19] ECM also provides mechanical strain for traction and orientation for angiogenic microvessels.[11−14] Previous studies have highlighted the importance of the stiffness and degradation effect of ECM on morphogenesis

Received: April 13, 2016
Accepted: July 11, 2016
Published: July 11, 2016

DOI: 10.1021/acsami.6b04431
ACS Appl. Mater. Interfaces 2016, 8, 19245−19255

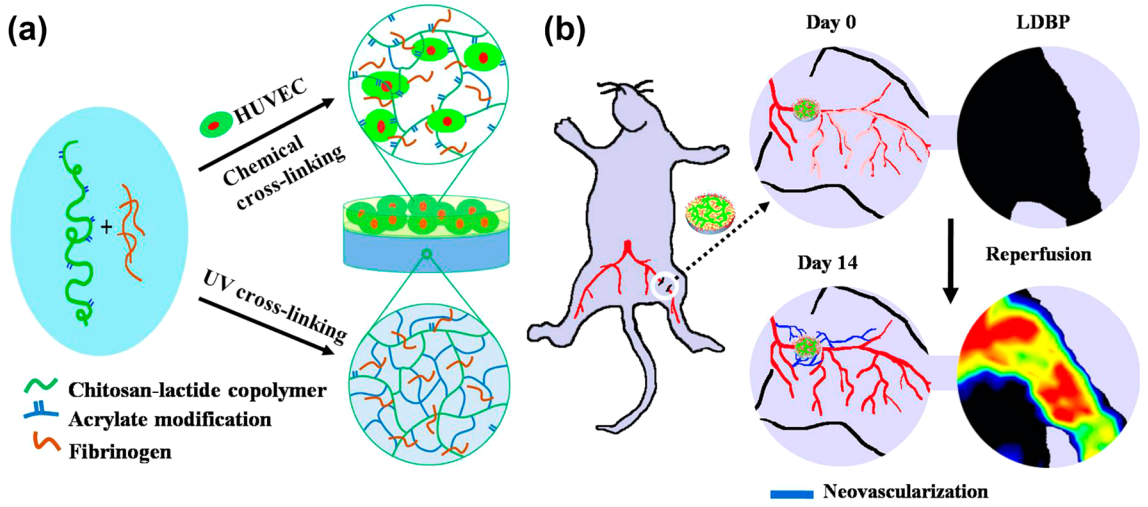

Figure 1. Design and schematic drawing of the hydrogel based-HUVEC aggregates. (a) Construction of a dual-layer hydrogel consisting of a cell-laden soft top layer and an acellular stiffer bottom layer. Biodegradable chitosan–lactide hydrogel was manipulated according to its elastic modulus and proteolytic degradation via chemically cross-linked or photo-cross-linking methods. (b) In vivo evaluation of the HUVEC aggregate-induced microvascular networks in a hind-limb ischemic model. Laser Doppler blood perfusion (LDBP) was performed between 0 and 14 days postsurgery to investigate whether the HUVEC aggregate-induced microvascular networks improves reperfusion rates in an ischemic hind limb.

and tubulogenesis of ECs.[3,10,11] For example, ECs have a tendency either not to form or to very slowly form tubular networks on relatively stiff and nondegradable matrixes because cell–ECM interactions are stronger than cell–cell contact.[11−13] On the other hand, a relatively soft, fast degradable matrix readily facilitates tube formation due to enhanced cell–cell contact, but the initially formed tubular structures easily regress during proteolytic degradation of the ECM.[7−13,20−23] Therefore, controlling interactions between cells and ECM is important to promote angiogenic sprouting, capillary formation, and vascular stability.[14,17−19,24] These processes can be well-orchestrated by regulating composition, physicochemical properties, and degradation of ECM.[11−13,20−23]

Recent studies have demonstrated that three-dimensional (3D) self-assembled cell aggregates can improve angiogenic activity by synthesizing and organizing ECM molecules. They can balance cell–cell and cell–ECM interactions and facilitate transmission of physiological information,[6,25−27] precondition themselves to ischemic environments during in vitro preculture periods, and secrete antiapoptotic factors.[6,25] Thus, the cells in the aggregates become more resistant to hypoxia and circumvent the occurrence of anoikis.[6,26]

Here, we report EC aggregate-induced microvascular networks to increase blood perfusion rate in a mouse model of hind-limb ischemia. In previous studies, we developed a chitosan–lactide hydrogel system that can be chemically cross-linked or photo-cross-linked with tunable elastic modulus and proteolytic degradation rate, and these hydrogels have been used to deliver growth factors to promote tissue regeneration in vivo.[28−30] In the present study, we engineered a dual-layer chitosan–lactide hydrogel consisting of a human umbilical vein endothelial cell (HUVEC)-laden, relatively soft, chemically cross-linked top layer and an acellular, relatively stiff, photo-cross-linked bottom layer. We hypothesize that the chemically cross-linked hydrogel will promote self-assembly of HUVEC aggregates, while the photo-cross-linked hydrogel will maintain structural integrity of the cell aggregate-induced microvascular networks. We further hypothesize that our innovative design will allow the HUVEC aggregate-induced microvascular networks to enhance blood perfusion rate in vivo.

2. MATERIALS AND METHODS

2.1. Materials. Chitosan, dimethyl sulfoxide, tin(II) 2-ethylhexanoate, triethylamine, methacrylic anhydride, and sodium metabisulfite were obtained from Sigma-Aldrich (St. Louis). D,L-Lactide was purchased from Ortec (Piedmont, SC). Human fibrinogen plasminogen depleted was used from Enzyme Research Laboratories (South Bend, IN). All other chemicals were used as received.

2.2. Fabrication of Chitosan–Lactide Hydrogels. The chitosan–lactide prepolymer solution was prepared as described in our previous studies.[28,29] To produce cross-linked hydrogel networks, sodium metabisulfite was mixed with the prepolymer solution to form a chemically cross-linked hydrogel (relatively soft), while a filtered photoinitiator solution (Irgacure 2959) was mixed to the prepolymer solution that was then exposed to 6.9 mW/cm^2 UV light to form a photo-cross-linked hydrogel (relatively stiff).

2.3. Characterization of Chitosan–Lactide Hydrogels. As described in previous studies,[28,29] we characterized the properties of the hydrogels in terms of mechanical stiffness, microstructure, and degradation. Compressive modulus of the hydrogels was measured to determine the stiffness of hydrogels (chemically cross-linked or photo-cross-linked). The microstructures and degradation profiles of the hydrogels were investigated to understand physicochemical properties of the hydrogels.

2.4. Cell Culture. Green fluorescent protein (GFP) expressing HUVECs were received from the laboratory of the late Dr. J. Folkman (Children's Hospital, Boston). They were cultured in EBM-2 (Lonza, Walkersville, MD) containing supplements from EGM-2 kit, 10% fetal bovine serum, and 1% penicillin streptomycin glutamine.

2.4.1. Metabolic Activity of HUVECs in the Chitosan–Lactide Hydrogels. An MTS assay was performed to test the cytotoxicity of the hydrogels and cell morphological changes in response to the hydrogels were also monitored using a Zeiss Axiovert 200 (Carl Zeiss Microimaging, Thornwood, NY) as described in previous methods.[29] Both the chemically cross-linked and photo-cross-linked hydrogels were evaluated with both indirect and direct contact cultures. First, indirect contact culture was performed to investigate the effect of the hydrogels on cellular metabolic activity through cell culture media. Initially, 50 000 cells were seeded and cultured for 3 days. The same number of cells was also directly cultured into a chemically cross-linked hydrogel or a photo-cross-linked hydrogel for 3 days. The

DOI: 10.1021/acsami.6b04431
ACS Appl. Mater. Interfaces 2016, 8, 19245−19255

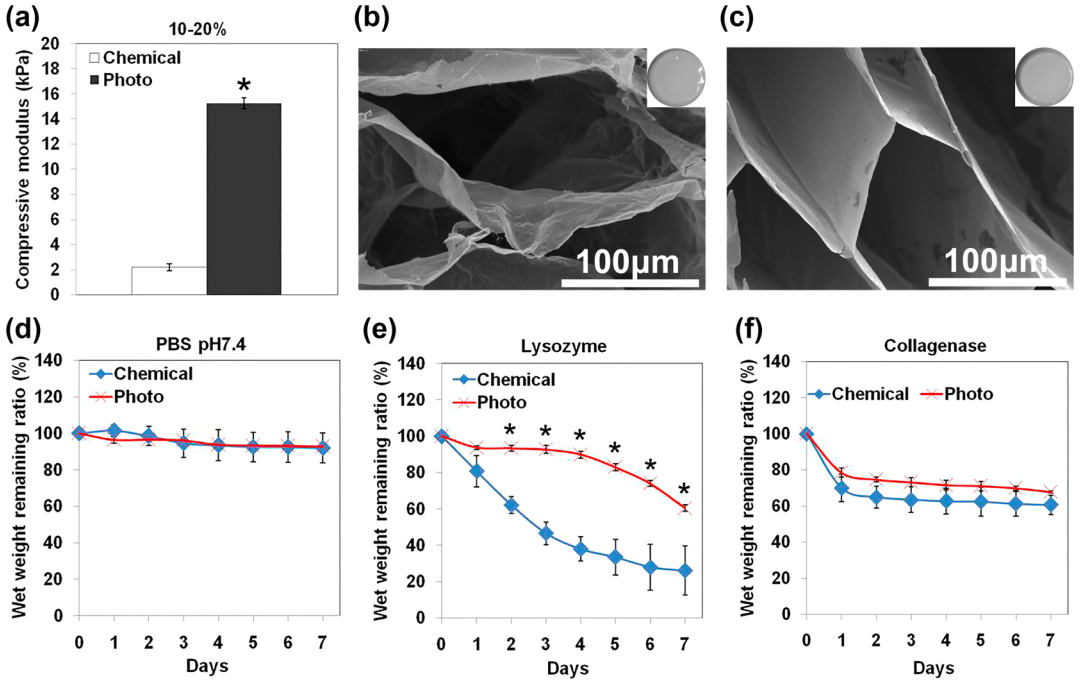

Figure 2. Characterization of the chitosan−lactide hydrogels. (a) Compressive modulus of chemically cross-linked or photo-cross-linked hydrogels. Unconfined compression tests were performed using an Instron 5944 materials testing system fitted with a 10 N load cell. The compressive modulus was determined for strain ranges of 10−20% from linear curve fits of the stress−strain curve. Representative SEM micrographs on the cross section of the freeze-dried hydrogel formed by (b) chemical cross-linking; (c) UV cross-linking. In vitro degradation of the hydrogels in (d) PBS (pH 7.4), (e) PBS (pH 7.4) containing lysozyme (100 μg/mL), and (f) PBS (pH 7.4) containing collagenase A (1 mg/mL) at 37 °C for 7 days. The degradation profile of the hydrogels was determined by measuring the wet weight remaining ratio of the hydrogels at each time point. Each value represents the mean ± SD (n = 3). * denotes significant difference between groups ($p < 0.05$).

number of viable cells was determined using an MTS assay. Photomicrographs of cells were also obtained.

2.4.2. Morphogenesis of HUVECs in the Chitosan−Lactide Hydrogels. We also monitored angiogenic characteristics of HUVECs in the chitosan−lactide hydrogels and compared them against HUVECs grown on tissue culture plastics. To evaluate the effect of 3D hydrogels on microvascular network formation, 5000 GFP-expressing HUVECs were cultured in tissue culture plastics or encapsulated into the chemically cross-linked hydrogels. GFP images of endothelial network formation were taken at day 1 and day 3. Five images of each sample were randomly taken with 10× objectives with Zeiss Axiovision software and quantified with NIH ImageJ software according to the following tube formation parameters: (1) total number of branches/mm^2 and (2) total length of branches in μm/mm^2. Angiogenic events of the HUVECs were also observed and imaged during 3 days of incubation.

2.4.3. MMP Activities of HUVECs Associated with Stiffness and Degradation of the Hydrogels. We investigated MMP-mediated degradation in response to cellular activities on the different hydrogels. We evaluated the level of MMP activities of HUVECs during cell culture periods of 3 days. 50 000 cells were seeded on the surface of chemically cross-linked or photo-cross-linked hydrogels and then cultured for 3 days. We then selected MMP-2 and MMP-10 as the index proteins, affecting degradation of ECM proteins during capillary tube formation and regression, respectively. The levels of MMP-2 and MMP-10 in the media were measured at day 3 using ELISA (Calbiochem, NJ) according to manufacturer's instructions. In addition, atomic force microscopy (AFM) was used to determine the local mechanical stiffness of the hydrogels affected by the cellular activities. The elasticity determination was done with a Park NX-10 in liquid cell with phosphate buffered saline (PBS). Curve analysis was conducted with SPIP software from Image Metrology A/S.

2.5. Engineering and Evaluation of a Dual-Layer Hydrogel Construct. We designed a dual-layer hydrogel construct to facilitate the formation of lasting EC aggregate-induced microvascular networks. As shown Figure 1a, the dual-layer hydrogel consists of a HUVEC-laden, relatively soft, chemically cross-linked top layer and an acellular, relatively stiff, photo-cross-linked bottom layer. The cell-encapsulated top layer was designed to promote self-assembly of HUVEC aggregates, while the bottom layer was designed to retain structural integrity of cell aggregates and cell-generated ECM.

2.5.1. Immunofluorescence Analysis. To study the ECM components and cell adhesion molecules in the HUVEC aggregate-induced microvascular networks, immunofluorescent staining was performed. In brief, 50 000 cells were suspended in a prepolymer solution which was then chemically cross-linked on top of the photo-cross-linked hydrogels, after which EGM-2 was added. The cells in the hydrogels were cultured in 24-well plates to form HUVEC aggregates for 7 days. Collagen IV and fibronectin as biomarkers of ECM components and vascular endothelial (VE) cadherin as a biomarker of a cell adhesion molecule were immunofluorescent-stained. Rabbit anticollagen IV, antifibronectin, and anti-VE cadherin were used as primary antibodies in 0.1% BSA and incubated overnight at 4 °C. Alexa Fluor 647 was used as secondary antibodies in 0.1% BSA−PBS and was incubated in the dark at room temperature for 1 h. Finally, 4′,6-diamidino-2-phenylindole (DAPI, 5 mg/mL) or Hoechst 33258 was used for staining the nuclei of the cells. The fluorescent images were obtained with a Zeiss Axiovert 200 microscope (Carl Zeiss Microimaging, Thornwood, NY).

2.5.2. Animal Study. The efficacy of the HUVEC aggregate-induced microvascular networks was evaluated using a hind-limb ischemia model. The schematic of the in vivo study is shown in Figure 1b. All procedures were approved by the Institutional Animal Care and Use Committee (IACUC) of Stanford University. BALB/c null/null male nude mice at 7−8 weeks of age were purchased from Charles River Laboratories (Wilmington, MA) and were maintained under standard conditions and diet. Five animals per group were used in this study. The ligation of the femoral artery was performed as described in previous study.[31] Briefly, mice were anesthetized with 1.5% isoflurane-O_2, and the hind limbs were depilated. After administration of

DOI: 10.1021/acsami.6b04431
ACS Appl. Mater. Interfaces 2016, 8, 19245−19255

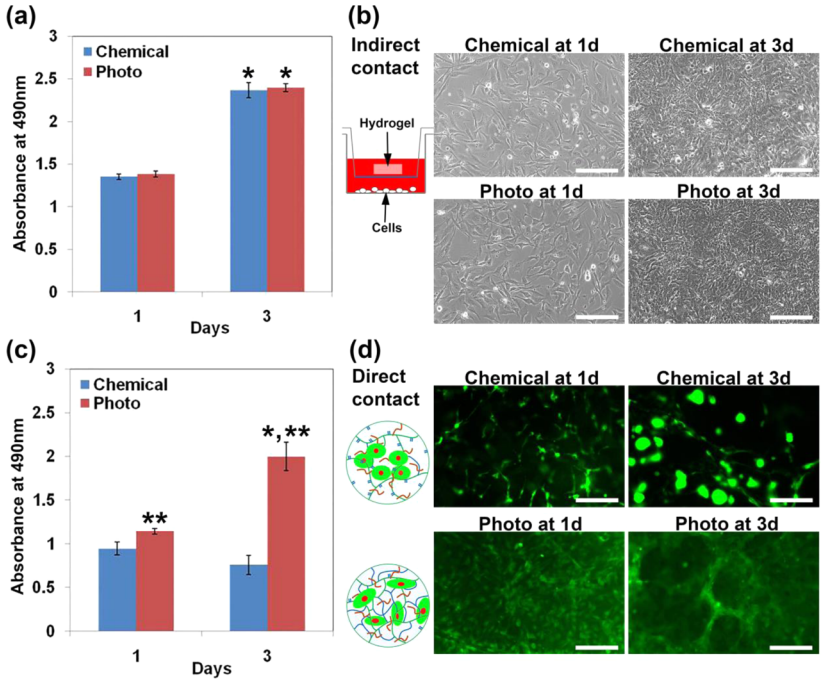

Figure 3. Viability of HUVECs in the chitosan−lactide hydrogels. (a) HUVECs were cultured via indirect contact and (b) their photomicrographs were processed. BD BioCoat control cell culture inserts (24 well, 8 μm pores) were used to evaluate the effect of the hydrogels on cell viability and proliferation through cell culture media at day 1 and day 3. (c) HUVECs were cultured via direct contact on the hydrogels and (d) GFP images of the cells were taken at day 1 and day 3. Initially, 50 000 of GFP expressing HUVECs were cultured and the number of viable cells was determined at day 1 and day 3 quantitatively using a MTS assay according to the manufacturer's instructions. The light absorbance at 490 nm was recorded using a micro plate reader (TECAN Infinite F50). * denotes significant difference between time points ($p < 0.05$). ** denotes significant difference between groups ($p < 0.05$).

buprenorphine (0.01 mg/kg intramuscular) as a pre-emptive analgesic, a 1 cm skin incision was made on the left thigh and the left femoral artery was exposed. After the superficial epigastric artery (SEA) was identified, the common femoral artery was ligated with two 7-0 ligatures placed proximal to the SEA. The artery was then transected between the sutures and separated 2−3 mm. The right legs were left intact to serve as control references. After femoral artery excision surgery, the mice received either no treatment, HUVECs-loaded hydrogels (5×10^5 cells per hydrogel), or the HUVEC aggregate-induced microvascular networks in hydrogels at the site of the femoral artery region. Initially, 1.5×10^5 cells were cultured for 5 days to form the HUVEC aggregate-induced microvascular networks. The wound was irrigated with sterile saline and closed, and cefazolin (50 mg/kg im) was administered. Under 1.5% isoflurane-O_2 anesthesia, non-invasive perfusion imaging of the hind limb was performed at 1, 3, 7, 10, and 14 days postsurgery. A PeriScan PIM 3 Imager (Perimed AB, Stockholm, Sweden) was used to evaluate the blood perfusion to the ischemic hind limb. The perfusion ratio (ischemic/nonischemic) in the limb of each animal was taken (foot to proximal ligation).

2.6. Statistical Analysis. Significant differences among different groups and experimental time points were analyzed by one-way ANOVA test. All data were considered statistically significant if $p < 0.05$. All measurements were presented as mean ± standard deviation.

3. RESULTS

3.1. Chemically Cross-Linked Chitosan−Lactide Hydrogel Demonstrating Lower Stiffness and Higher Degradation Rate Compared to the Photo-Cross-Linked One. Unconfined compression tests revealed the effect of chemical cross-linking and photo-cross-linking methods on stiffness of the hydrogels (Figure 2a). The average compressive modulus for the photo-cross-linked hydrogel that was 15.3 ± 0.9 kPa was significantly greater than the modulus for the chemically cross-linked hydrogel at 2.2 ± 0.5 kPa ($p < 0.05$).

Scanning electron microscopy (SEM) images show the cross-sectional area of freeze-dried hydrogels by chemical cross-linking or photo-cross-linking, respectively (Figure 2b,c). Both hydrogels were microporous, but displayed different morphology. The softer, chemically cross-linked hydrogel exhibited relatively thinner and rougher porous structure compared to the stiffer, photo-cross-linked hydrogel. It indicates greater cross-linked networks by photo-cross-linking parameters via UV exposure on the prepolymer solution than chemical cross-linking.

We examined the wet remaining ratios of the hydrogels to evaluate the effect of enzymatic activities on the degradation behavior of hydrogels by incubating them in solutions with pH 7.4 at 37 °C of PBS, 100 μg/mL lysozyme, or 1 mg/mL collagenase A (Figure 2d−f). In the PBS medium, the wet weight remaining ratios decreased similarly for the soft, chemically cross-linked and stiff, photo-cross-linked hydrogels, dropping to 92% and 93.2% of the original wet weight remaining ratios, respectively, after 1 week of incubation. In the 100 μg/mL lysozyme, the weight remaining ratios decreased to 26.1% for the soft, chemically cross-linked and 60.4% for the stiff, photo-cross-linked hydrogel after a week of incubation, respectively, due to lysozyme-regulated hydrolysis. In the 1 mg/mL collagenase A, the weight remaining ratios decreased to 70.1% for the soft, chemically cross-linked and 78.5% for the stiff, photo-cross-linked hydrogel after day 1 and then slowly decreased over a week of incubation. In both the lysozyme- and collagenase A-containing solutions, the degradation rate of the stiff, photo-cross-linked hydrogel was significantly slower than that of the soft, chemically cross-linked one ($p < 0.05$). Thus, we conclude that the soft, chemically cross-linked hydrogels are

DOI: 10.1021/acsami.6b04431
ACS Appl. Mater. Interfaces 2016, 8, 19245−19255

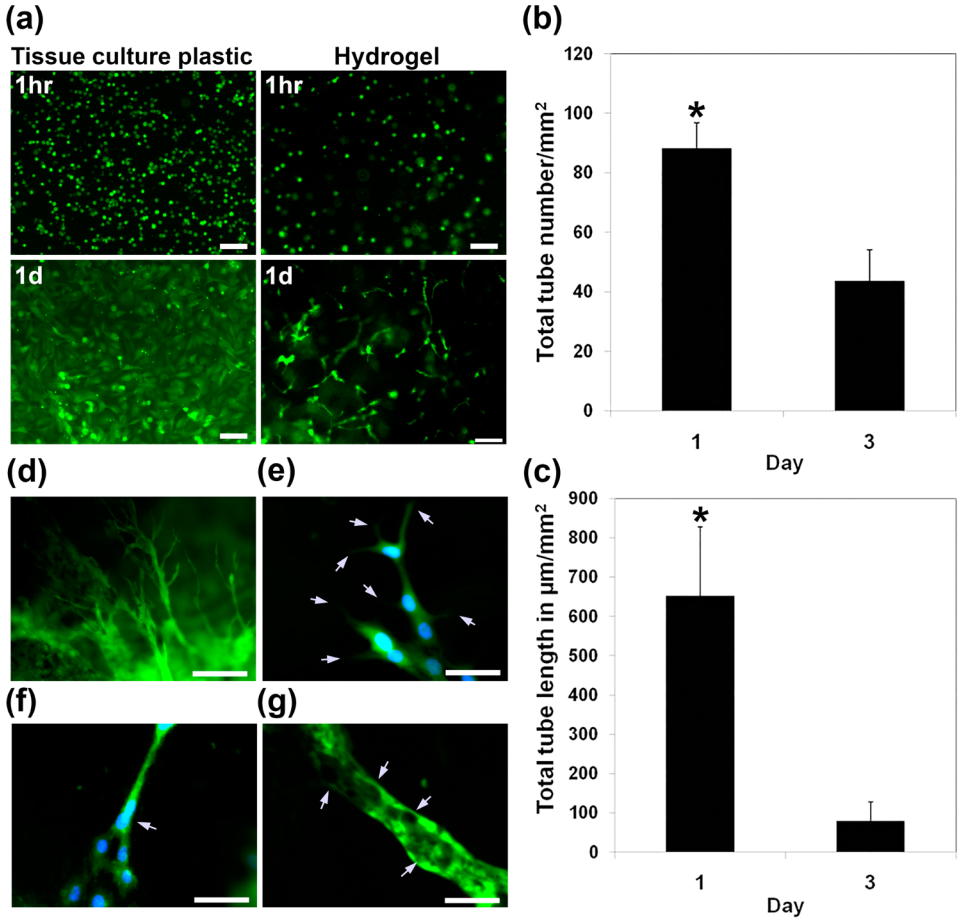

Figure 4. Morphogenesis and tubulogenesis of HUVECs in the chitosan−lactide hydrogels. (a) The effect of 3D hydrogels on microvascular network formation was monitored by culturing 5000 cells on tissue culture plastics or encapsulating them into the soft and fast degradable chitosan−lactide hydrogels. In addition, GFP images of endothelial network formation in the hydrogels were taken at day 1and day 3. Five images of each sample were randomly taken with 10× objectives using a software (Zeiss, AxioVision) and quantified with NIH ImageJ software according to the following tube formation parameters: (b) total tube number (total number of tubes/mm^2) and (c) total tube length (total length of tubes in μm/mm^2). GFP images of HUVECs cultured in the hydrogels showed (d) ECs sprouting (bar = 200 μm), (e) outgrowth of an endothelial tip cell (arrows indicate filopodia, bar = 50 μm), (f) stalk cell proliferation (arrow indicates growing stalk cells, bar = 50 μm), and (g) lumen formation (arrow indicates coalescence of intracellular vacuoles, bar = 100 μm). * denotes significant difference between groups ($p < 0.05$).

more susceptible to enzymatic activities compared to the stiff, photo-cross-linked hydrogels.

3.2. HUVECs Are Viable in Both the Chemically Cross-Linked and Photo-Cross-Linked Chitosan−Lactide Hydrogels. The cytotoxicity of the hydrogels was evaluated by quantifying cell metabolic activity via an MTS assay before the construction of a dual-layer hydrogel. Figure 3a showed no significant difference in metabolic activity of HUVECs between groups via indirect cell culture, but there were significantly increased metabolic activities for both groups during 3 days of in vitro culture ($p < 0.05$). This result indicated that the cells were able to grow and proliferate regardless of the cross-linking methods (Figure 3b). Direct contact culture between groups for 3 days of incubation further supported biocompatibility of the stiff, photo-cross-linked hydrogels ($p < 0.05$). Metabolic activity of HUVECs on the stiff, slowly degradable, photo-cross-linked hydrogels significantly increased during day 3 of incubation compared with day 1 (Figure 3c, $p < 0.05$). However, cell metabolic activity in the soft, quickly degradable, chemically cross-linked hydrogels did not show significant increase between day 1 and day 3 incubations. As shown in Figure 3d, the morphology of cells and microvessels in direct cell culture on the two hydrogel groups correlated with the cellular metabolic activities in Figure 3c, with cells preferring to aggregate on the soft matrix and spread on the stiff one.

3.3. Morphogenesis of HUVECs in the Chitosan−Lactide Hydrogels. Figure 4a shows microscopic observation of HUVECs cultured in the tissue culture plastics and encapsulated into the soft chitosan−lactide hydrogel. On tissue culture plastic, which is substantially stiffer and nondegradable compared to the hydrogels, HUVECs proliferated to become confluent without network formation by day 1 of incubation. Upon encapsulation of cells into the hydrogels, HUVECs showed distinct morphological changes including cell elongation, branching, and network formation at day 1 of incubation (Figure 4a). The total number and total length of branching networks in the hydrogels significantly decreased at day 3 compared with day 1 (Figure 4b,c, $p < 0.05$), as cells aggregated. GFP images show that HUVECs cultured in the hydrogels exhibited endothelial sprouting and branching (Figure 4d), including outgrowth of endothelial tip cells (Figure 4e), and growing stalk cells (Figure 4f). The tip cells were located at the forefront of vessel branches and had numerous filopodia responding to angiogenic stimuli, while the

DOI: 10.1021/acsami.6b04431
ACS Appl. Mater. Interfaces 2016, 8, 19245−19255

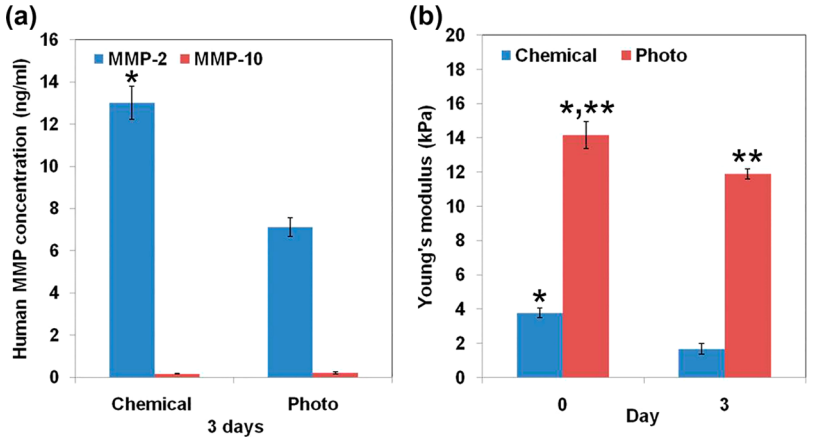

Figure 5. MMP activity of HUVECs associated with stiffness and degradation of the hydrogels. Initially 50 000 of GFP expressing HUVECs were cultured on the surface of chemically cross-linked or photo-cross-linked hydrogels for 3 days. (a) Levels of MMP-2 and MMP-10 of HUVECs. The concentration of the MMPs in the media was measured at day 3 using ELISA kits according to manufacturer's instructions. (b) Local mechanical stiffness of the hydrogels affected by the cellular activities using AFM. * denotes significant difference between time points ($p < 0.05$). ** denotes significant difference between groups ($p < 0.05$).

stalk cells that followed the leading tip cell proliferated and elongated. Figure 4g indicates the lumen formation by coalescence of intracellular vacuoles, which further interconnected with neighboring vacuoles. However, these angiogenic events were not lasting due to proteloytic degradation of the chitosan−lactide hydrogels.

3.4. Increased MMP-2 Activities of HUVECs Are Associated with Increased Vessel Formation and Degradation of the Hydrogel Substrate. We further investigated MMP activities of HUVECs in response to the properties of the hydrogels and evaluated the changes in stiffness of the hydrogels accordingly. The amount of MMP-2 was significantly higher on the soft, chemically cross-linked hydrogels than on the stiffer, photo-cross-linked hydrogels at day 3 ($p < 0.05$), while those of MMP-10 were relatively very low and similar between hydrogels at day 3 (Figure 5a). Given that high MMP-2 levels of HUVECs support vessel formation, the MMP activities closely align with our observation that the soft, chemically cross-linked hydrogel promoted network formation more strongly than the stiff, photo-cross-linked one.

This study also demonstrates that increased MMP-2 activity can influence local degradation of the hydrogel substrate. Figure 5b shows the changes in mechanical stiffness of the hydrogels affected by the cellular activities using AFM. Initial average Young's modulus was 3.8 ± 0.3 and 14.2 ± 0.8 kPa for chemically cross-linked and photo-cross-linked hydrogels, respectively. During 3 days of in vitro HUVECs culture, Young's modulus significantly decreased to 1.7 ± 3.1 and 11.9 ± 0.3 kPa, respectively ($p < 0.05$). While Young's modulus of both hydrogels significantly decreased at day 3 compared with day 0 ($p < 0.05$), the Young's modulus of the soft, chemically cross-linked samples decreased approximately 55% compared to 16% for the photo-cross-linked samples ($p < 0.05$). The decreases in Young's modulus of both hydrogels are most likely associated with the expression of MMPs that causes degradation of hydrogels.

3.5. Engineering a Dual-Layer Hydrogel Construct for HUVEC Aggregate-Induced Microvascular Networks. *3.5.1. Immunofluorescence Analysis.* As shown in Figure 6a, we designed a dual-layer hydrogel construct to promote the formation of a lasting HUVEC aggregate-induced microvascular network by combining a cell-laden soft, chemically cross-linked hydrogel top layer with an acellular, photo-cross-linked stiffer bottom layer. By day 3 of cell culture, proteolytic degradation of the soft, chemically cross-linked hydrogel induced the rapid formation of HUVEC aggregates, while the stiffer bottom layer provided a stable substrate and retained structural integrity of HUVEC aggregates. Over time, individual HUVEC aggregates extended endothelial sprouts and grew toward neighboring aggregates to establish complex anastomosing microvascularized networks. After day 7 of cell culture, we investigated the presence of ECM components and cell adhesion molecules with immunofluorescent staining. As shown in Figure 6b−d, the enriched vascular endothelial (VE) cadherin, fibronectin, and collagen type IV accumulated and coexisted within the HUVEC aggregate-induced microvascular networks.

3.5.2. Animal Studies. The effectiveness of the HUVEC aggregate-induced microvascular networks on blood flow restoration was tested in male nude mice (BALB/c null/null) that were subjected to femoral artery ligation. We compared the improvement in reperfusion rates of the HUVEC aggregate-induced microvascular networks against no treatment and HUVEC-loaded hydrogels. At 0, 1, 3, 7, 10, and 14 days postsurgery, we quantitatively evaluated blood perfusion to the hind limb using the laser Doppler perfusion imaging (LDPI) system. As shown in Figure 7, the mice receiving the HUVEC aggregate-induced microvascular networks showed a significant increase in perfusion ratio (ischemic/control hind limb) compared with the no treatment group and the HUVECs-loaded hydrogels ($p < 0.05$), and the levels of necrosis were reduced. However, we did not observe any significant difference in blood flow rate between the no treatment group and the HUVECs-loaded hydrogels. All three groups revealed some degree of toe necrosis. However, the HUVEC aggregate-induced microvascular network group did not require toe amputation, while 60% and 20% of the animals in the no treatment group and the HUVEC-loaded hydrogel group, respectively, did (Table 1). This result indicates that the HUVEC aggregate-induced microvascular networks accelerated the blood flow rate due to their therapeutic capability to restore perfusion in vivo.

DOI: 10.1021/acsami.6b04431
ACS Appl. Mater. Interfaces 2016, 8, 19245−19255

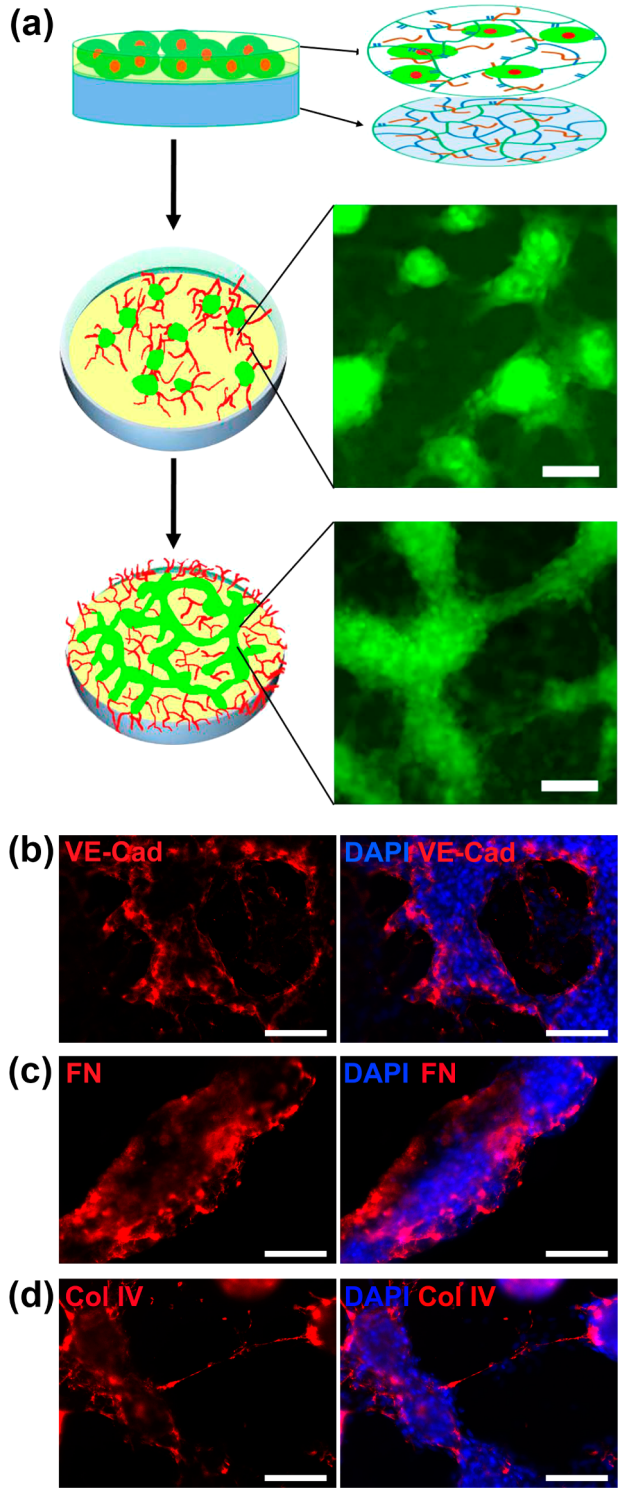

Figure 6. Immunofluorescence analysis of ECM components and cell adhesion molecules in the HUVEC aggregate-induced microvascular networks. (a) The HUVEC aggregates were constructed by combining a cell-laden soft top layer with an acellular stiffer bottom layer and cultured for 7 days in vitro. After about 3 days of cell culture, HUVEC aggregates were formed via proteolytic degradation of the soft hydrogel, while the stiffer bottom layer supported structural integrity and retained angiogenic properties of HUVECs. After 7 days of cell culture, the presence of (b) VE-cadherin (VE-Cad), (c) fibronectin (FN), and (d) collagen type IV (Col IV) was evaluated by using immunofluorescent staining methods. Cell nuclei were counterstained with DAPI. (Bar = 100 μm).

4. DISCUSSION

Recent studies have shown that prevascularized tissue constructs can accelerate angiogenic processes, restore vascular function, and improve engraftment.[5,32] Prevascularization strategies aim to establish functional microvascular networks in vitro before implantation.[5,6,25−27,32] In this study, we have shown that engineering a dual-layer hydrogel construct can create HUVEC aggregate-induced microvascular networks in vitro and promote reperfusion in a mouse model of hind-limb ischemia in vivo. In our previous studies, we developed a biocompatible, biodegradable chitosan−lactide hydrogel.[28−30] The properties of the chitosan−lactide hydrogels including mechanical stiffness and degradation were tunable by controlling different ratios of the copolymer and cross-linking degree and using different cross-linking methods.[28,29] The fibrinogen molecules have also been introduced into the copolymer networks to promote cell attachment, enhance growth factor binding, and increase susceptibility to proteolytical degradation to regenerate tissue in vivo.[29,30,33]

In this study, we modulated stiffness and enzymatic degradation of the chitosan−lactide hydrogels by using different cross-linking methods. Accordingly, we prepared the photo-cross-linked hydrogel that was relatively stiff (E = ∼15 kPa) and slowly degradable, and the chemically cross-linked hydrogel that was relatively soft (E = ∼2 kPa) and quickly degradable. MTS assay via the indirect and direct contact cultures suggested that both hydrogels were nontoxic. The indirect contact culture showed that the cells could grow and proliferate regardless of the cross-linking methods. Via direct contact culture, however, we observed a significant difference in metabolic activity of HUVECs between groups. There was no increase in metabolic activity of HUVECs in the soft hydrogel at day 3 compared with that at day 1 because its fast degradation induced cell detachment and loss unlike that in the stiff hydrogel. Instead, as shown in Figure 3d, the soft hydrogels promoted cell−cell interactions and self-assembly of the cells into capillary-like structures within day 1 of incubation. It is likely that the cells experienced less resistance from the softer hydrogel and readily self-assembled themselves into the branching structures. At day 3, the cells formed larger aggregates in accordance with degradation of the hydrogel. In contrast, the stiff hydrogels enhanced cell−substrate interactions and cell spreading, and delayed the formation of capillary-like structures until the hydrogels became less stiff via degradation.[21,22] At day 3, loop structures gradually appeared. The differences in cell morphology and vascular development reflect the fact that the cells appear to be highly migratory when in contact with a stiffer matrix. However, when the matrix becomes less stiff due to cell-mediated degradation over time, the cell−matrix interactions become weaker, causing cells to accumulate and form aggregates, branching, and loop structures.

Consistent with previous studies,[19,24,34] HUVECs expressed different amounts of MMP-2 and MMP-10 in response to different degrees of stiffness of the hydrogels. These MMPs are important factors for the degradation of various types of ECM proteins during capillary tube formation and regression, respectively.[19,24,34−36] In this study, the amounts of MMP-2 were significantly higher on the relatively soft hydrogels than on the stiffer hydrogels. These cellular activities, in turn, significantly decreased the local mechanical stiffness of the hydrogels due to degradation of hydrogels. Our findings

DOI: 10.1021/acsami.6b04431
ACS Appl. Mater. Interfaces 2016, 8, 19245−19255

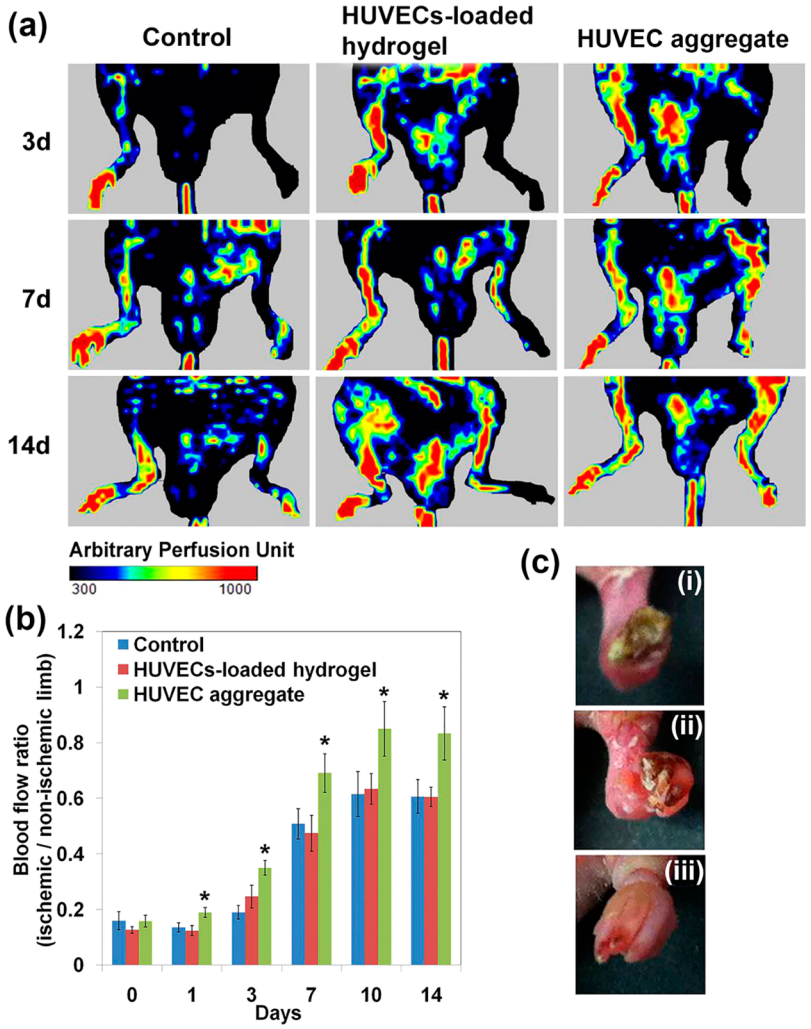

Figure 7. Hind-limb perfusion in nude mice with ligated femoral artery. (a) Representative LDPI images of ischemic hind limbs as a function of time postsurgery, corresponding to treatment conditions: no treatment, HUVECs-loaded hydrogel, and HUVEC aggregate-induced microvascular networks. (b) Quantification of perfusion ratio (ischemic/normal leg) at days 0, 1, 3, 7, 10, and 14 postsurgery (n = 5). (c) Gross photographs of toe necrosis at day 7 responding to the conditions: (i) no treatment; (ii) HUVECs-loaded hydrogel; (iii) HUVEC aggregate-induced microvascular networks. * denotes significant difference between groups (p < 0.05).

Table 1. Quantification of Hind-Limb Ischemia Severity at 2 Weeks Postsurgery (n = 5)

samples	no treatment	HUVECs-loaded hydrogel	HUVEC aggregate-induced microvascular networks
amputation	3/5 (60%)	1/5 (20%)	0/5 (0%)
toe necrosis	2/5 (40%)	4/5 (80%)	2/5 (40%)
normal	0/5 (0%)	0/5 (0%)	3/5 (60%)

suggest increased expression of MMPs is very closely related to degradation of the hydrogel barriers, further affecting cell behaviors such as cell attachment, migration, and invasion.[37−39] Thus, controlling microenvironments with different degrees of stiffness and degradation of the matrix seems to be one of the key factors to regulate functions of EC.

Our findings on the correlation among EC morphogenesis, hydrogel stiffness, and degradation inspired us to design a dual-layer hydrogel construct for the fast formation of the lasting HUVEC aggregate-induced microvascular networks (Figure 8). The fast formation of HUVEC aggregates was induced by MMP-mediated degradation of the soft top layer. The lasting nature was enabled by the stiff, slowly degradable hydrogel, which reduced proteolysis, and provided a stable template for the retention of VE cadherin, and accumulation of fibronectin and Col IV as well as the structural integrity. In addition, previous studies have demonstrated that the MMPs secreted by the cells actively participate in synthesis of the ECM components during ECM remodeling.[24,34,35,40] The ECM assembly is affected by properties of biomaterials because cells rearrange the ECM proteins at the material interface.[17,40−43] In particular, the deposition of fibronectin on the surface of the materials affects vascular development and stability.[35,41,42] As such, our dual-layer hydrogel approach successfully created a favorable microenvironment for neovascularization.

Lastly, we evaluated the effectiveness of the HUVEC aggregate-induced microvascular networks on blood flow rates in a mouse model of hind-limb ischemia. Blood perfusion to the hind limb was found to be the greatest in mice that received the HUVEC aggregate-induced microvascular networks. The HUVEC aggregate group also reduced limb necrosis and amputation. These results suggest that the increased perfusion rate is ascribed to the fast restoration of blood flow because the

DOI: 10.1021/acsami.6b04431
ACS Appl. Mater. Interfaces 2016, 8, 19245−19255

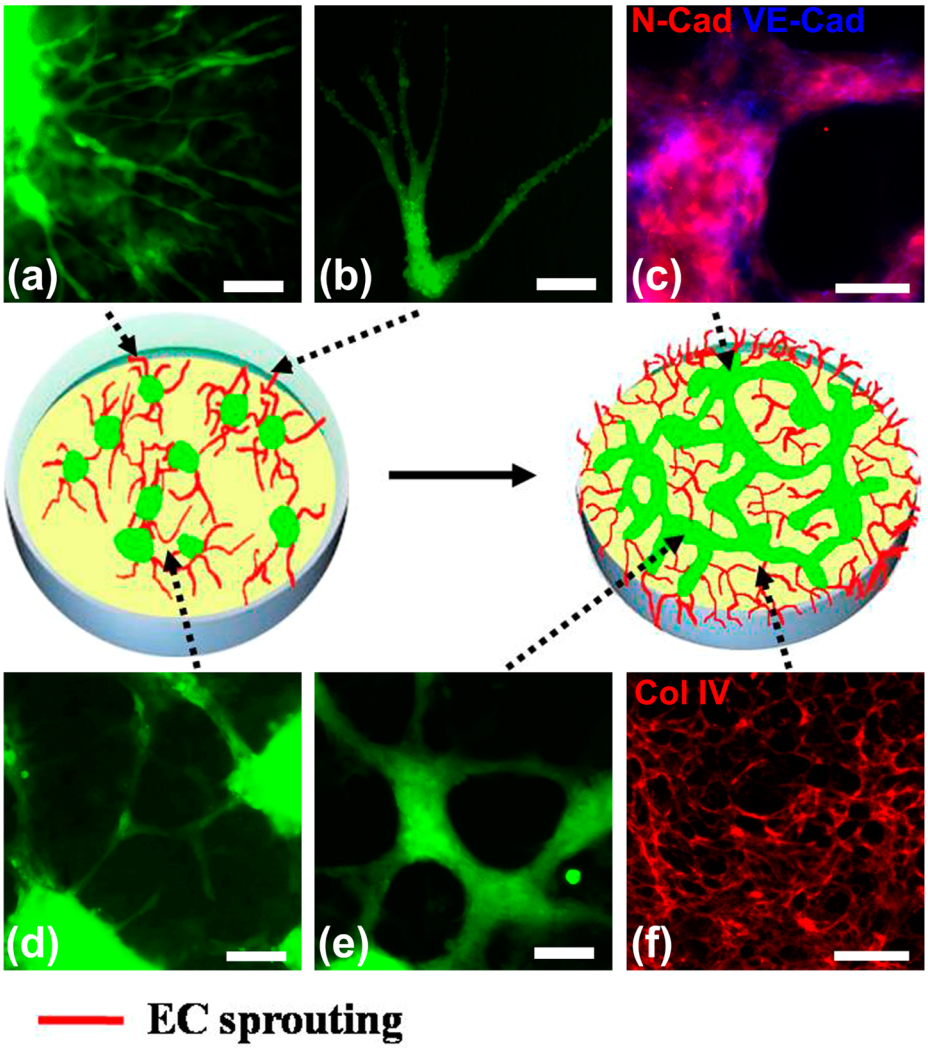

Figure 8. In vitro development and angiogenic characteristics of the HUVEC aggregate-induced microvascular networks. HUVEC aggregates were formed via proteolytic degradation of the soft top layer, while the stiffer bottom layer supported structural integrity and retained angiogenic properties of HUVECs. Green fluorescent protein (GFP) images of HUVECs showed the major step of angiogenesis in the HUVEC aggregate-induced microvascular networks, including (a) EC sprouting (bar = 100 μm), (b) tip cell formation (bar = 20 μm), (c) cell adhesion molecules (N-Cad (red) and VE-Cad (yellow), bar = 50 μm), and (d) branching (bar = 100 μm). Capillary sprouts originating from the HUVEC aggregates grew toward neighboring aggregates to extend (e) complex anastomosing networks (bar = 100 μm). (f) Enriched, stabilized structural ECM components (Col IV (red), bar = 50 μm) in the HUVEC aggregates maintained cell viability and enhanced angiogenesis in the HUVEC aggregate disk.

preformed and functionally stable vasculature can induce rapid anastomosis with host collateral vessels and enhance angiogenesis compared with the cells individually growing in the hydrogel in vivo.

In addition, therapeutic angiogenesis can be enhanced by controlling material components and degradation.[44,45] Previous studies have demonstrated that therapeutic efficacy of fibrinogen can be improved by combining it with biomaterials that can maintain biological functionality and structural support.[44,45] In our previous study,[29] the photo-cross-linked chitosan−lactide hydrogel combined with fibrinogen molecules showed slow degradation and induced bone regeneration with low risk of inflammation in a rat femoral bone defect model. In another study, we have also demonstrated that the delivery of heparin binding-epidermal growth factor like growth factor (HB-EGF) via the chemically cross-linked chitosan−lactide hydrogel could accelerate the healing of chronic tympanic membrane perforations in mouse models.[30] It also restored the normal histological structure and completely degraded without causing hearing loss. As such, we have shown that the chitosan−lactide hydrogels are an effective delivery system for tissue regeneration without inflammation. In the present study, our findings support the strategy of prevascularized tissue engineering, which appropriately regulates the functionality and the in vivo fate of the cells.[1−5] The HUVEC aggregates can be formed via MMP-mediated fast degradation, while accumulated cell-generated ECM that is continuously remodeled by cells in vitro remains on the surface of the hydrogels due to slow degradation of the hydrogels. In this way, we could enhance therapeutic efficacy without any adverse side effects during the experimental periods. In future studies, we will further confirm the direct blood flow after spontaneous anastomosis between the prevascularized and host vessels using animal models, such as cranial window and dorsal skinfold chamber models.[46,47]

5. CONCLUSION

In the present study, we have shown that a dual-layer approach of chitosan−lactide hydrogels with different degrees of stiffness

DOI: 10.1021/acsami.6b04431
ACS Appl. Mater. Interfaces 2016, 8, 19245−19255

and degradation rate can be used to construct the HUVEC aggregate-based microvascular networks, which then accelerate blood perfusion rate in a mouse model of hind-limb ischemia. This study has demonstrated that control over cell−cell and cell−ECM interactions via different properties of biomaterials can promote EC functionality. In the future, we will further develop this technology to even more closely mimic microenvironments for vascular network formation.

AUTHOR INFORMATION

Corresponding Author

*Y.Y.: Department of Orthopedic Surgery, Stanford University, 300 Pasteur Drive, Edwards R155, Stanford, CA 94305. Tel.: 650-723-0772. Fax: 650-724-5401. E-mail: ypyang@stanford.edu.

Author Contributions

S.K. designed and performed experiments, analyzed data, and wrote the paper; T.K. performed animal surgery and analyzed data; D.W. performed AFM, analyzed data, and wrote the paper; Y.Y. provided overall guidance, designed experiments, and wrote the paper.

Notes

The authors declare no competing financial interest.

ACKNOWLEDGMENTS

The authors thank Drs. Joseph C. Wu and Nigel Kooreman in the Department of Medicine (Cardiology) and Department of Radiology (Molecular Imaging Program) at the Stanford University School of Medicine for their support with LDBP imaging. This work was partially funded by grants from DOD PRORP W81XWH-10-1-0966, Airlift Research Foundation (W81XWH-10-200-10), Wallace H. Coulter Foundation, NIH R01AR057837 from NIAMS, and NIH R01DE021468 from NIDCR.

REFERENCES

(1) Phelps, E. A.; Landázuri, N.; Thulé, P. M.; Taylor, W. R.; García, A. J. Bioartificial Matrices for Therapeutic Vascularization. *Proc. Natl. Acad. Sci. U. S. A.* **2010**, *107*, 3323−3328.

(2) Cho, S. W.; Moon, S. H.; Lee, S. H.; Kang, S. W.; Kim, J.; Lim, J. M.; Kim, H. S.; Kim, B. S.; Chung, H. M. Improvement of Postnatal Neovascularization by Human Embryonic Stem Cell derived Endothelial-like Cell Transplantation in a Mouse Model of Hind-limb Ischemia. *Circulation* **2007**, *116*, 2409−2419.

(3) Lutolf, M. P.; Hubbell, J. A. Synthetic Biomaterials as Instructive Extracellular Microenvironments for Morphogenesis in Tissue Engineering. *Nat. Biotechnol.* **2005**, *23*, 47−55.

(4) Sacchi, V.; Mittermayr, R.; Hartinger, J.; Martino, M. M.; Lorentz, K. M.; Wolbank, S.; Hofmann, A.; Largo, R. A.; Marschall, J. S.; Groppa, E.; Gianni-Barrera, R.; Ehrbar, M.; Hubbell, J. A.; Redl, H.; Banfi, A. Long-lasting Fibrin Matrices Ensure Stable and Functional Angiogenesis by Highly Tunable, Sustained Delivery of Recombinant VEGF164. *Proc. Natl. Acad. Sci. U. S. A.* **2014**, *111*, 6952−6957.

(5) Krishnan, L.; Willett, N. J.; Guldberg, R. E. Vascularization Strategies for Bone Regeneration. *Ann. Biomed. Eng.* **2014**, *42*, 432−444.

(6) Chen, D. Y.; Wei, H. J.; Lin, K. J.; Huang, C. C.; Wang, C. C.; Wu, C. T.; Chao, K. T.; Chen, K. J.; Chang, Y.; Sung, H. W. Three-dimensional Cell Aggregates Composed of HUVECs and cbMSCs for Therapeutic Neovascularization in a Mouse Model of Hindlimb Ischemia. *Biomaterials* **2013**, *34*, 1995−2004.

(7) Aplin, A. C.; Zhu, W. H.; Fogel, E.; Nicosia, R. F. Vascular Regression and Survival are Differentially Regulated by MT1-MMP and TIMPs in the Aortic Ring Model of Angiogenesis. *Am. J. Physiol. Cell. Physiol.* **2009**, *297*, C471−C480.

(8) Hanjaya-Putra, D.; Bose, V.; Shen, Y. I.; Yee, J.; Khetan, S.; Fox-Talbot, K.; Steenbergen, C.; Burdick, J. A.; Gerecht, S. Controlled Activation of Morphogenesis to Generate a Functional Human Microvasculature in a Synthetic Matrix. *Blood* **2011**, *118*, 804−815.

(9) Mercado-Pagán, Á. E.; Stahl, A.; Shanjani, Y.; Yang, Y. Vascularization in Bone Tissue Engineering Constructs. *Ann. Biomed. Eng.* **2015**, *43*, 718−729.

(10) Ingber, D. E. Mechanical Signaling and the Cellular Response to Extracellular Matrix in Angiogenesis and Cardiovascular Physiology. *Circ. Res.* **2002**, *91*, 877−887.

(11) Sieminski, A. L.; Hebbel, R. P.; Gooch, K. J. The Relative Magnitudes of Endothelial Force Generation and Matrix Stiffness Modulate Capillary Morphogenesis In Vitro. *Exp. Cell Res.* **2004**, *297*, 574−584.

(12) Kniazeva, E.; Putnam, A. J. Endothelial Cell Traction and ECM Density Influence Both Capillary Morphogenesis and Maintenance in 3-D. *Am. J. Physiol. Cell. Physiol.* **2009**, *297*, C179−C187.

(13) Yamamura, N.; Sudo, R.; Ikeda, M.; Tanishita, K. Effects of the Mechanical Properties of Collagen Gel on the In Vitro Formation of Microvessel Networks by Endothelial Cells. *Tissue Eng.* **2007**, *13*, 1443−1453.

(14) Davis, G. E.; Senger, D. R. Endothelial Extracellular Matrix: Biosynthesis, Remodeling, and Functions during Vascular Morphogenesis and Neovessel Stabilization. *Circ. Res.* **2005**, *97*, 1093−1107.

(15) Laurie, G. W.; Leblond, C. P.; Martin, G. R. Localization of Type IV Collagen, Laminin, Heparan Sulfate Proteoglycan, and Fibronectin to the Basal Lamina of Basement Membranes. *J. Cell Biol.* **1982**, *95*, 340−344.

(16) Dickinson, L. E.; Moura, M. E.; Gerecht, S. Guiding Endothelial Progenitor Cell Tube Formation using Patterned Fibronectin Surfaces. *Soft Matter* **2010**, *6*, 5109−5119.

(17) Coelho, N. M.; Salmerón-Sánchez, M.; Altankov, G. Fibroblasts Remodeling of Type IV Collagen at a Biomaterials Interface. *Biomater. Sci.* **2013**, *1*, 494−502.

(18) Visse, R.; Nagase, H. Matrix Metalloproteinases and Tissue Inhibitors of Metalloproteinases: Structure, Function, and Biochemistry. *Circ. Res.* **2003**, *92*, 827−839.

(19) Ehrbar, M.; Sala, A.; Lienemann, P.; Ranga, A.; Mosiewicz, K.; Bittermann, A.; Rizzi, S. C.; Weber, F. E.; Lutolf, M. P. Elucidating the Role of Matrix Stiffness in 3D Cell Migration and Remodeling. *Biophys. J.* **2011**, *100*, 284−293.

(20) Pelham, R. J., Jr.; Wang, Y. l. Cell Locomotion and Focal Adhesions are Regulated by Substrate Flexibility. *Proc. Natl. Acad. Sci. U. S. A.* **1997**, *94*, 13661−13665.

(21) Reinhart-King, C. A.; Dembo, M.; Hammer, D. A. Cell-cell Mechanical Communication through Compliant Substrates. *Biophys. J.* **2008**, *95*, 6044−6051.

(22) Califano, J. P.; Reinhart-King, C. A. A Balance of Substrate Mechanics and Matrix Chemistry Regulates Endothelial Cell Network Assembly. *Cell. Mol. Bioeng.* **2008**, *1*, 122−132.

(23) Reinhart-King, C. A.; Dembo, M.; Hammer, D. A. The Dynamics and Mechanics of Endothelial Cell Spreading. *Biophys. J.* **2005**, *89*, 676−689.

(24) Ghajar, C. M.; Blevins, K. S.; Hughes, C. C.; George, S. C.; Putnam, A. J. Mesenchymal Stem Cells Enhance Angiogenesis in Mechanically Viable Prevascularized Tissues via Early Matrix Metalloproteinase Upregulation. *Tissue Eng.* **2006**, *12*, 2875−2888.

(25) Bhang, S. H.; Lee, S.; Lee, T. J.; La, W. G.; Yang, H. S.; Cho, S. W.; Kim, B. S. Three-dimensional Cell Grafting Enhances the Angiogenic Efficacy of Human Umbilical Vein Endothelial Cells. *Tissue Eng., Part A* **2012**, *18*, 310−319.

(26) Lee, W. Y.; Chang, Y. H.; Yeh, Y. C.; Chen, C. H.; Lin, K. M.; Huang, C. C.; Chang, Y.; Sung, H. W. The Use of Injectable Spherically Symmetric Cell Aggregates Self-assembled in a Thermoresponsive Hydrogel for Enhanced Cell Transplantation. *Biomaterials* **2009**, *30*, 5505−5513.

(27) Napolitano, A. P.; Chai, P.; Dean, D. M.; Morgan, J. R. Dynamics of the Self-assembly of Complex Cellular Aggregates on

DOI: 10.1021/acsami.6b04431
ACS Appl. Mater. Interfaces 2016, 8, 19245−19255

Micromolded Nonadhesive Hydrogels. *Tissue Eng.* **2007**, *13*, 2087−2094.
(28) Kim, S.; Kang, Y.; Mercado-Pagán, Á. E.; Maloney, W. J.; Yang, Y. In Vitro Evaluation of Photo-crosslinkable Chitosan-Lactide Hydrogels for Bone Tissue Engineering. *J. Biomed. Mater. Res., Part B* **2014**, *102*, 1393−1406.
(29) Kim, S.; Bedigrew, K.; Guda, T.; Maloney, W. J.; Park, S.; Wenke, J. C.; Yang, Y. P. Novel Osteoinductive Photo-cross-linkable Chitosan-Lactide-Fibrinogen Hydrogels Enhance Bone Regeneration in Critical Size Segmental Bone Defects. *Acta Biomater.* **2014**, *10*, 5021−5033.
(30) Santa-Maria, P. L.; Kim, S.; Varsak, Y. K.; Yang, Y. P. Heparin Binding -Epidermal Growth Factor Like Growth Factor for Regeneration of Chronic Tympanic Membrane Perforations in Mice. *Tissue Eng., Part A* **2015**, *21*, 1483−1494.
(31) Couffinhal, T.; Silver, M.; Zheng, L. P.; Kearney, M.; Witzenbichler, B.; Isner, J. M. Mouse Model of Angiogenesis. *Am. J. Pathol.* **1998**, *152*, 1667−1679.
(32) Chen, X.; Aledia, A. S.; Ghajar, C. M.; Griffith, C. K.; Putnam, A. J.; Hughes, C. C.; George, S. C. Prevascularization of a Fibrin-based Tissue Construct Accelerates the Formation of Functional Anastomosis with Host Vasculature. *Tissue Eng., Part A* **2009**, *15*, 1363−1371.
(33) Martino, M. M.; Briquez, P. S.; Ranga, A.; Lutolf, M. P.; Hubbell, J. A. Heparin-Binding Domain of Fibrin(ogen) Binds Growth Factors and Promotes Tissue Repair When Incorporated within a Synthetic Matrix. *Proc. Natl. Acad. Sci. U. S. A.* **2013**, *110*, 4563−4568.
(34) Liu, H.; Chen, B.; Lilly, B. Fibroblasts Potentiate Blood Vessel Formation Partially through Secreted Factor TIMP-1. *Angiogenesis* **2008**, *11*, 223−234.
(35) Shi, F.; Sottile, J. MT1-MMP Regulates the Turnover and Endocytosis of Extracellular Matrix Fibronectin. *J. Cell Sci.* **2011**, *124*, 4039−4050.
(36) Saunders, W. B.; Bayless, K. J.; Davis, G. E. MMP-1 Activation by Serine Proteases and MMP-10 Induces Human Capillary Tubular Network Collapse and Regression in 3D Collagen Matrices. *J. Cell Sci.* **2005**, *118*, 2325−2340.
(37) Kaufman, D. A.; Albelda, S. M.; Sun, J.; Davies, P. F. Role of Lateral Cell-cell Border Location and Extracellular/Transmembrane Domains in PECAM/CD31 Mechanosensation. Biochem. Biophys. *Biochem. Biophys. Res. Commun.* **2004**, *320*, 1076−1081.
(38) Galbraith, C. G.; Yamada, K. M.; Sheetz, M. P. The Relationship between Force and Focal Complex Development. *J. Cell Biol.* **2002**, *159*, 695−705.
(39) Osawa, M.; Masuda, M.; Kusano, K.; Fujiwara, K. Evidence for a Role of Platelet Endothelial Cell Adhesion Molecule-1 in Endothelial Cell Mechanosignal Transduction: Is It a Mechanoresponsive Molecule? *J. Cell Biol.* **2002**, *158*, 773−85.
(40) Llopis-Hernández, V.; Rico, P.; Ballester-Beltrán, J.; Moratal, D.; Salmerón-Sánchez, M. Role of Surface Chemistry in Protein Remodeling at the Cell-material Interface. *PLoS One* **2011**, *6*, e19610.
(41) Wijelath, E. S.; Murray, J.; Rahman, S.; Patel, Y.; Ishida, A.; Strand, K.; Aziz, S.; Cardona, C.; Hammond, W. P.; Savidge, G. F.; Rafii, S.; Sobel, M. Novel Vascular Endothelial Growth Factor Binding Domains of Fibronectin Enhance Vascular Endothelial Growth Factor Biological Activity. *Circ. Res.* **2002**, *91*, 25−31.
(42) Sottile, J.; Hocking, D. C. Fibronectin Polymerization Regulates the Composition and Stability of Extracellular Matrix Fibrils and Cell-matrix Adhesions. *Mol. Biol. Cell* **2002**, *13*, 3546−3559.
(43) Stevens, M. M.; George, J. H. Exploring and Engineering the Cell Surface Interface. *Science* **2005**, *310*, 1135−1138.
(44) Santos, S. G.; Lamghari, M.; Almeida, C. R.; Oliveira, M. I.; Neves, N.; Ribeiro, A. C.; Barbosa, J. N.; Barros, R.; Maciel, J.; Martins, M. C.; Gonçalves, R. M.; Barbosa, M. A. Adsorbed Fibrinogen Leads to Improved Bone Regeneration and Correlates with Differences in the Systemic Immune Response. *Acta Biomater.* **2013**, *9*, 7209−7217.
(45) Mountziaris, P. M.; Spicer, P. P.; Kasper, F. K.; Mikos, A. G. Harnessing and Modulating Inflammation in Strategies for Bone Regeneration. *Tissue Eng., Part B* **2011**, *17*, 393−402.
(46) Cheng, G.; Liao, S.; Wong, H. K.; Lacorre, D. A.; di Tomaso, E.; Au, P.; Fukumura, D.; Jain, R. K.; Munn, L. L. Engineered Blood Vessel Networks Connect to Host Vasculature via Wrapping-and-tapping Anastomosis. *Blood* **2011**, *118*, 4740−4749.
(47) Gibot, L.; Galbraith, T.; Huot, J.; Auger, F. A. A Preexisting Microvascular Network Benefits In Vivo Revascularization of a Microvascularized Tissue-engineered Skin Substitute. *Tissue Eng., Part A* **2010**, *16*, 3199−3206.

DOI: 10.1021/acsami.6b04431
ACS Appl. Mater. Interfaces 2016, 8, 19245−19255